Nuclear Engineering and Technology 53 (2021) 3151–3157

Contents lists available at ScienceDirect

Nuclear Engineering and Technology

journal homepage: www.elsevier.com/locate/net

Original Article

Copper neutron transport libraries validation by means of a ^{252}Cf standard neutron source

Martin Schulc*, Michal Košťál, Evžen Novák, Jan Šimon

Research Centre Rez Ltd, 250 68, Husinec-Řež 130, Czech Republic

ARTICLE INFO

Article history:
Received 8 January 2021
Received in revised form
9 April 2021
Accepted 26 April 2021
Available online 7 May 2021

Keywords:
Copper cross sections
^{252}Cf
IRDFF-II
Criticality safety

ABSTRACT

Copper is an important structural material in various nuclear energy applications, therefore the correct knowledge of copper cross sections is crucial. The presented paper deals with a validation of different copper transport libraries by means of activation of selected samples. An intense ^{252}Cf(sf) source with a reference neutron spectrum was used as a neutron source. After irradiation, the samples were measured using a high purity germanium detector and the dosimeter reaction rates were inferred. These experimental data were compared with MCNP6 calculations using CENDL-3.1, JENDL-4.0, ENDF/B-VII.1, ENDF/B-VIII.0, JEFF-3.2 and JEFF-3.3 evaluated Cu transport libraries. The experiment specifically focuses on ^{58}Ni(n,p)^{58}Co, ^{93}Nb(n,2n)^{92m}Nb, ^{197}Au(n,g)^{198}Au and ^{55}Mn(n,g)^{56}Mn dosimetry reactions. Evaluated activation cross sections of these dosimetric reactions were taken from the IRDFF-II library. The best library performance depends on the energy region of interest.

1. Introduction

One of the commonly used structural materials is copper. The correct evaluation of copper cross sections is complicated by the fact that natural copper is composed of two isotopes ^{63}Cu (69.15%) and ^{65}Cu (30.85%), both with high abundance. Copper is used not only in fusion facilities divertors, magnets, microwave waveguides and mirrors [1] but it is also an important structural component in spent fuel storage casks [2,3]. Thus good knowledge of copper cross section and decreasing of uncertainty in its description are important for better design of components mentioned above. The goal of the presented paper is to test various copper cross sections using the isotopic ^{252}Cf source. The ^{252}Cf source was chosen since it is a very well known reference neutron spectrum [4,5]. Therefore results using this source are loaded with lower uncertainties than validation efforts using other neutron sources [6].

2. Description of the experimental setup and evaluations

The isotopic ^{252}Cf source had an average total emission of 2.67E8 n/s during irradiation of niobium and nickel foils, and emission of 2.38E8 n/s during the irradiation of manganese and gold foils. The emission was calculated from the data in the Certificate of Calibration obtained from National Physical Laboratory, United Kingdom. The source was placed in the centre of the copper block. The block was composed of smaller copper plates, see Fig. 1. The assembled copper block has dimensions: 48 cm length, 49.5 cm width, and 49.5 cm height. Irradiation of the samples took almost 39 days uninterrupted. The entire copper block in the laboratory is displayed in Fig. 2, left. The activation foils were attached to the thin aluminium foil, see Fig. 2, right and placed into the copper block at the distance of 16 cm from the ^{252}Cf neutron source centre.

After the end of the irradiation, all irradiated samples were measured on the upper cap of the high purity germanium (HPGe) detector (ORTEC GM35P4) one by one. The detector efficiency was calculated using a computational MCNP6 model, see Ref. [7]. The experimental reaction rate q was derived from the peak of interest Net Peak Area using formula

$$q = \frac{C(T_m)\lambda T_m}{\eta\varepsilon N K T_l}\,\frac{1}{e^{-\lambda\Delta T}}\,\frac{1}{1-e^{-\lambda T_m}}\,\frac{1}{1-e^{-\lambda T_{irr}}}, \tag{1}$$

where: q is the experimental reaction rate per atom per second, N is the number of target isotope nuclei, η is the detector efficiency, ε is

* Corresponding author.
E-mail address: Martin.Schulc@cvrez.cz (M. Schulc).

https://doi.org/10.1016/j.net.2021.04.029

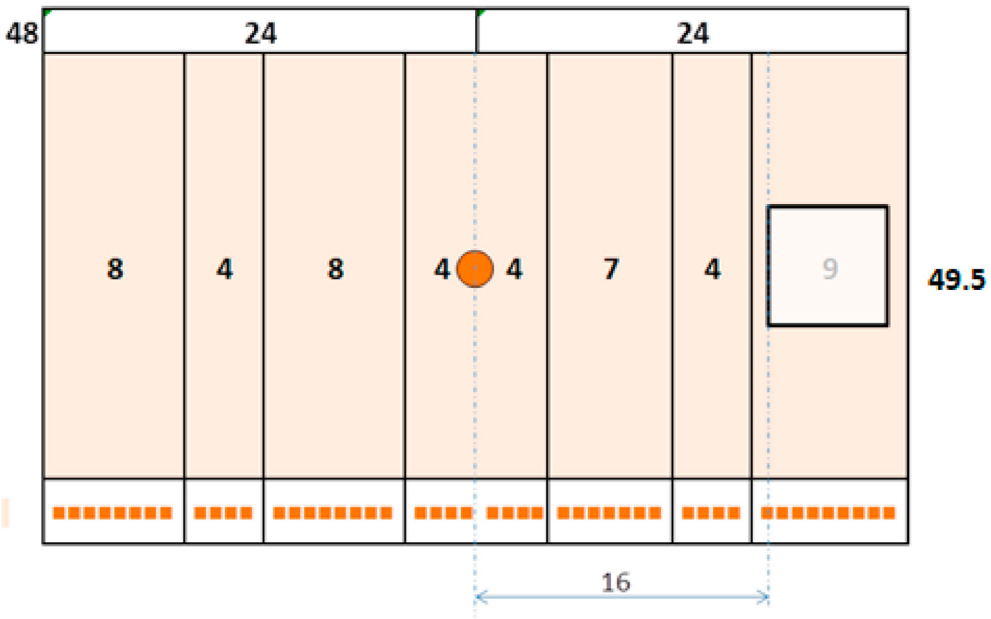

Fig. 1. Cross section of copper block. The activation foils were placed into the square gap 16 cm from the centre. All dimensions are in centimetres.

Fig. 2. Left: Copper block was used for the experiment. Right: activation foils holder made of aluminium.

the gamma branching ratio, λ is the decay constant, k characterizes the abundance of the isotope of interest in the target and its purity, ΔT is the time between the end of irradiation and the start of HPGe measurement, $C(T_m)$ is the measured number of counts per second, T_m is the real time of measurement by HPGe, T_l is the live time of measurement by HPGe (it is time of measurement corrected to the dead time of the detector) and T_{irr} is the time of irradiation. The parameters of irradiation and used constants are summarized in the following tables. Table 1 shows the activation products half-lifes, evaluated gamma energy lines, and gamma emission probabilities for all studied reactions. Table 2 summarizes the cooling times and HPGe measurement times for all activation products.

Table 1
Parameters of the investigated neutron-induced threshold reactions.

Reaction	Half-life	Gamma Energy [MeV]	Gamma emission probability
^{197}Au(n,g)^{198}Au	2.6941 days	0.411802	95.62%
^{58}Ni(n,p)^{58}Co	70.86 days	0.81076	99.45%
^{93}Nb(n,2n)^{92m}Nb	10.15 days	0.93444	99.15%
^{55}Mn(n,g)^{56}Mn	2.5789 h	0.8467638	98.85%

Table 2
Parameters of irradiation and following HPGe measurement.

Reaction	Irradiation time	Cooling time	Measurement time
^{197}Au(n,g)^{198}Au	7.50 days	49.99 h	1266 s
^{55}Mn(n,g)^{56}Mn	7.50 days	0.34 h	4.40 h
^{58}Ni(n,p)^{58}Co	38.93 days	310.67 h	2.18 h
^{93}Nb(n,2n)^{92m}Nb	38.93 days	5.87 h	208.25 h

Irradiation time was the same in all cases.

Fig. 3 shows the cross sections of the investigated dosimetric reactions in IRDFF-II library. These reactions are sensitive in the broad range of neutron energies, namely, ^{58}Ni(n,p)^{58}Co, ^{93}Nb(n,2n)^{92m}Nb, ^{197}Au(n,g)^{198}Au and ^{55}Mn(n,g)^{56}Mn. The niobium in the high energy region, nickel in the medium energy region and manganese and gold are sensitive in the region under 1 MeV. All reactions except ^{55}Mn(n,g)^{56}Mn reaction were validated in the ^{252}Cf neutron spectrum, see Refs. [8,9], and [10]. Fig. 4 compares the neutron spectra in the place of activation foils with the bare ^{252}Cf spectrum. Bare ^{252}Cf spectrum was multiplied by a constant to show the similarity of spectra above 3.0 MeV.

The relevant uncertainties that have been investigated were: uncertainties on the experimental positions of the samples, copper block density, emission of the source, the net peak area uncertainties measured by the HPGe detector, the detector efficiency uncertainty, density of the Pd matrix, position of the source, influence of ^{250}Cf, for details see Ref. [11]. Calculations were performed by means of the MCNP6 transport code [12] using various neutron transport libraries, i.e., ENDF/B-VIII.0 [13], ENDF/B-VII.1 [14], JEFF-3.3 [15], JEFF-3.2 [16], JENDL-4.0 [17] and CENDL-3.1 [18]. The cross sections of the activation reactions under study were taken from IRDFF-II [4] library. The ^{252}Cf(sf) reference neutron spectrum based on Mannhart evaluation [5] was taken from the IRDFF-II webpage (https://www-nds.iaea.org/IRDFF/IRDFF-II_sp_ENDF.zip). The calculation model was compiled from all available data (dimensions, densities, materials …). The activation foils were placed into MCNP6 model and were included in computational MCNP6 model.

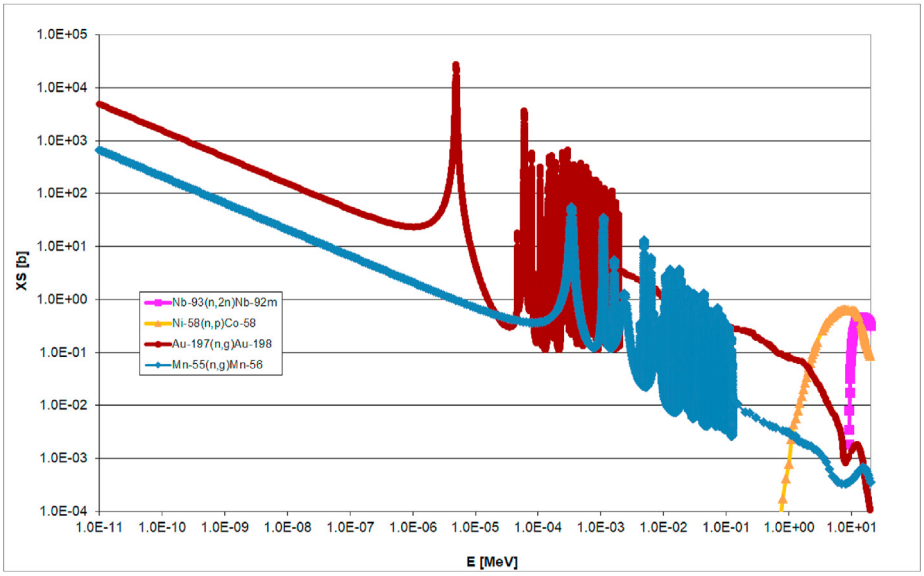

Fig. 3. Overview of studied reactions cross sections. Cross sections were taken from IRDFF-II library.

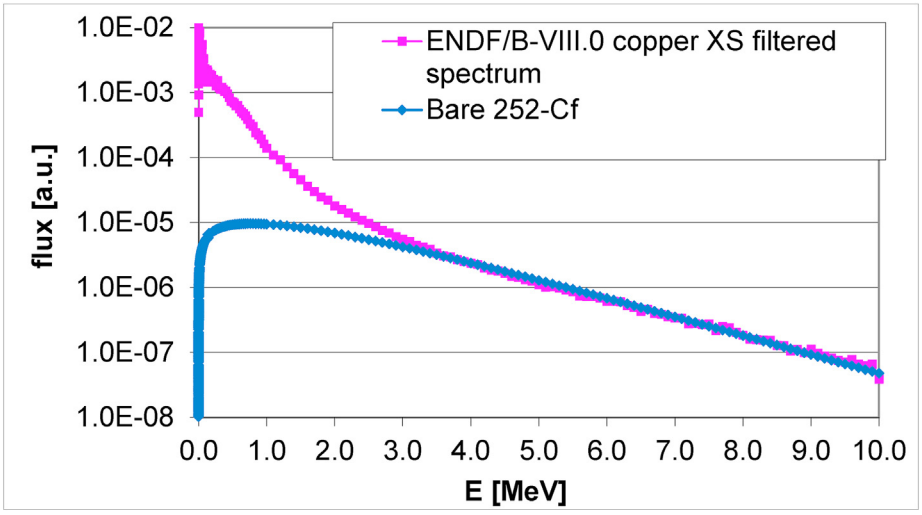

Fig. 4. Comparison of neutron spectra in the place of activation foils. The bare ^{252}Cf spectrum was multiplied by a constant to show the similarity of spectra above 3.0 MeV.

Table 3
Calculation and C/E-1 comparison for ^{58}Ni(n,p)^{58}Co reaction.

^{58}Ni(n,p)^{58}Co	q[s^{-1} atom^{-1} neutron^{-1}]	C/E-1	Uncertainty
EXPERIMENT	3.89E-30		4.1%
ENDF/B-VII.1	4.87E-30	25.33%	2.2%
ENDF/B-VIII.0	4.07E-30	4.09%	2.2%
JEFF-3.3	5.45E-30	39.96%	2.2%
JEFF-3.2	4.81E-30	24.03%	2.2%
JENDL-4.0	4.57E-30	17.45%	2.2%
CENDL-3.1	4.67E-30	20.16%	2.2%

Table 4
Calculation and C/E-1 comparison for ^{93}Nb(n,2n)^{92m}Nb reaction.

^{93}Nb(n,2n)^{92m}Nb	q[s^{-1} atom^{-1} neutron^{-1}]	C/E-1	Uncertainty
EXPERIMENT	3.14E-32		4.7%
ENDF/B-VII.1	3.06E-32	−2.59%	2.5%
ENDF/B-VIII.0	2.71E-32	−13.69%	2.5%
JEFF-3.3	3.88E-32	23.41%	2.5%
JEFF-3.2	3.05E-32	−3.05%	2.5%
JENDL-4.0	3.19E-32	1.61%	2.5%
CENDL-3.1	2.95E-32	−6.27%	2.5%

Table 5
Calculation and C/E-1 comparison for ^{197}Au(n,g)^{198}Au reaction.

^{197}Au(n,g)^{198}Au	q[s^{-1} atom^{-1} neutron^{-1}]	C/E-1	Uncertainty
EXPERIMENT	4.00E-28		3.9%
ENDF/B-VII.1	3.76E-28	−6.18%	2.1%
ENDF/B-VIII.0	3.69E-28	−7.81%	2.1%
JEFF-3.3	3.73E-28	−6.79%	2.1%
JEFF-3.2	3.80E-28	−5.22%	2.1%
JENDL-4.0	3.72E-28	−7.08%	2.1%
CENDL-3.1	3.58E-28	−10.59%	2.1%

Table 6
Calculation and C/E-1 comparison for ^{55}Mn(n,g)^{56}Mn reaction.

^{55}Mn(n,g)^{56}Mn	q[s^{-1} atom^{-1} neutron^{-1}]	C/E-1	Uncertainty
EXPERIMENT	1.94E-29		4.5%
ENDF/B-VII.1	1.91E-29	−1.36%	2.2%
ENDF/B-VIII.0	1.85E-29	−4.84%	2.2%
JEFF-3.3	1.89E-29	−2.71%	2.2%
JEFF-3.2	1.86E-29	−4.01%	2.2%
JENDL-4.0	1.88E-29	−2.83%	2.2%
CENDL-3.1	1.81E-29	−6.43%	2.2%

3. Results

Table 3 shows the results and comparisons for the ^{58}Ni(n,p)^{58}Co reaction. The agreement within uncertainties is achieved only in ENDF/B-VIII.0 library. Other libraries differ by approximately 20% except JEFF-3.3 which differs by almost 40%. Table 4 displays results for ^{93}Nb(n,2n)^{92m}Nb reaction. In this case, the agreement within uncertainties is achieved with ENDF/B-VII.1, JEFF-3.2, and JENDL-4.0 libraries. JEFF-3.3 differs by 23.41% and ENDF/B-VIII.0 by −13.69%. Concerning the ^{197}Au(n,g)^{198}Au reaction, the results are shown in Table 5. No library gives agreement within uncertainty. The best result is achieved using JEFF-3.2 library (difference −5.22%) and the worst with CENDL-3.1 library (−10.59% difference). Table 6 deals with ^{55}Mn(n,g)^{56}Mn reaction, agreement within uncertainties is achieved with all libraries except CENDL-3.1 and ENDF/B-VIII.0 library.

Big reaction rates differences among libraries are caused by big differences in elastic and inelastic cross sections for both ^{63}Cu and ^{65}Cu isotopes in the region above 1 MeV. ^{65}Cu(n,el) reaction has identical evaluation in JEFF-3.3 and JEFF-3.2 libraries. However, for inelastic reactions, JEFF-3.3 cross sections are substantially lowered in comparison to JEFF-3.2 for energies higher than 3 MeV. However, the C/E ratio is the worst in JEFF-3.3 for threshold reactions.

Following figures show comparisons of elastic and inelastic cross sections. Fig. 5 and Fig. 6 show ^{63}Cu(n,el) and ^{65}Cu(n,el) cross sections in various libraries, respectively. Fig. 7 and Fig. 8 display ^{63}Cu(n,inl) and ^{65}Cu(n,inl) cross sections in various libraries, respectively.

Fig. 9 and Fig. 10 show energy regions sensitivity to reactions under study in the copper block cavity.

The comparison of reaction rates allows to judge about the quality of the evaluated transport library for copper isotopes. Another crucial performance test is a criticality calculation involving copper reflector. Table 7 compares criticality calculations with ZEUS-1 benchmark experiment, case 1 (HEU-072-MET-FAST). The computational model was taken from ICSBEP database and only copper cross section were changed. Basic transport library employed in benchmark was ENDF/B-VI [19]. Only agreement with experiment was achieved using ENDF/B-VIII.0 library. This fact is supported by Ref. [20], where the copper sensitive benchmarks were selected and ENDF/B-VIII.0 library shows substantial

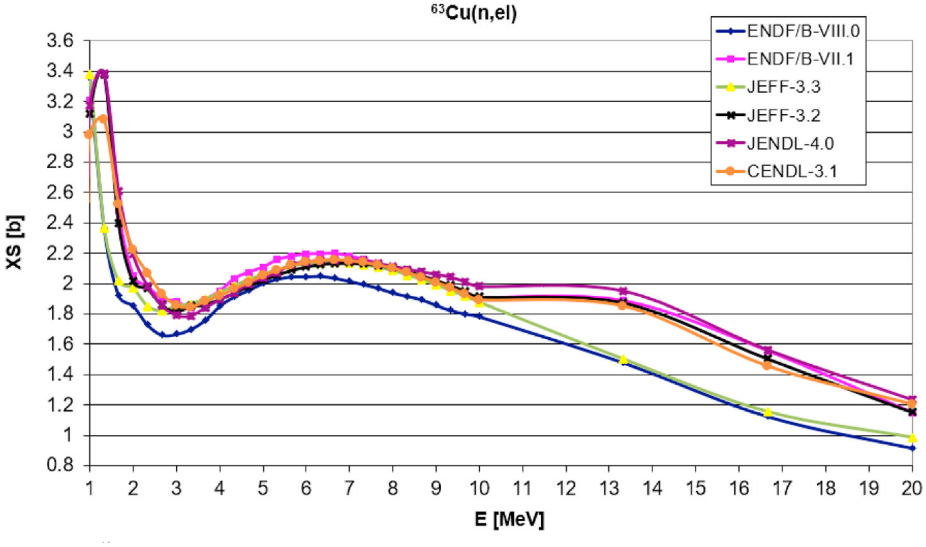

Fig. 5. ^{63}Cu(n,el) reaction cross section in different libraries.

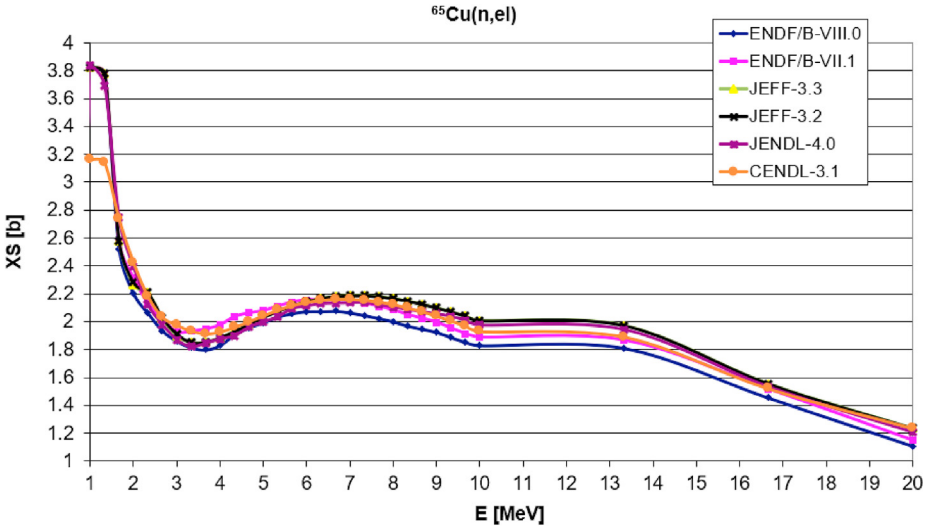

Fig. 6. ^{65}Cu(n,el) reaction cross section in different libraries.

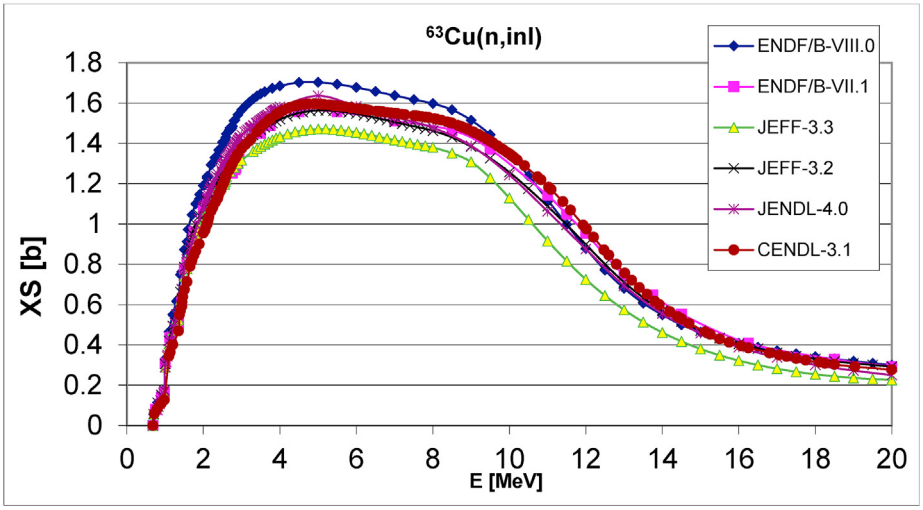

Fig. 7. ^{63}Cu(n,inl) reaction cross section in different libraries.

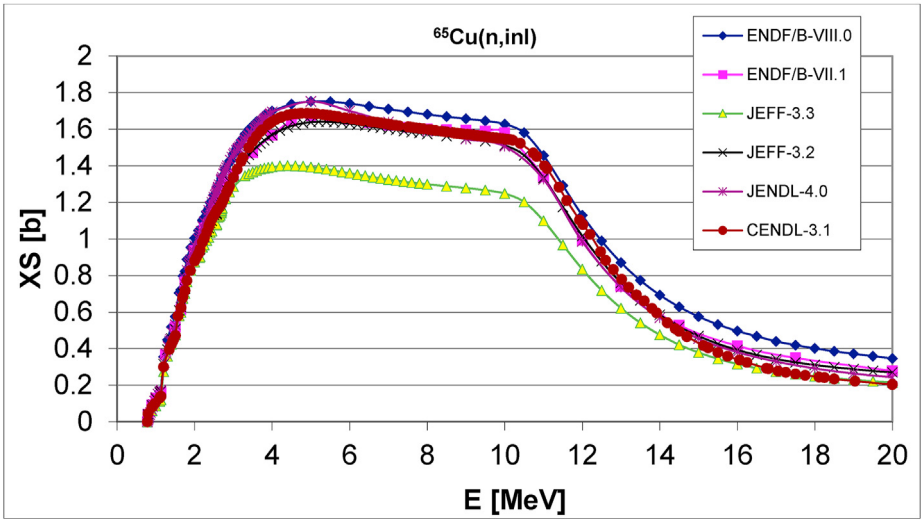

Fig. 8. ^{65}Cu(n,inl) reaction cross section in different libraries.

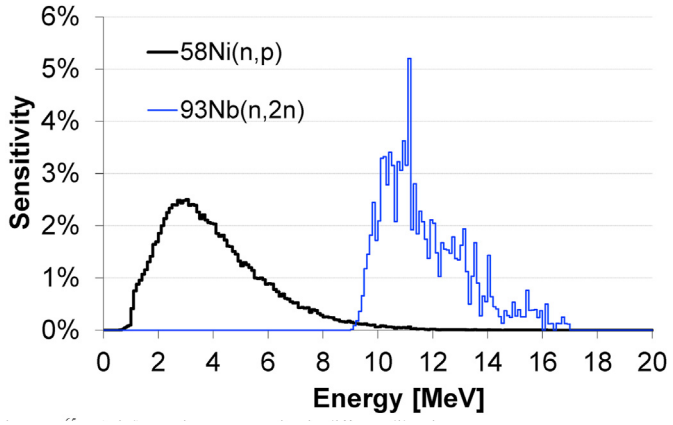

Fig. 9. ^{65}Cu(n,inl) reaction cross section in different libraries.

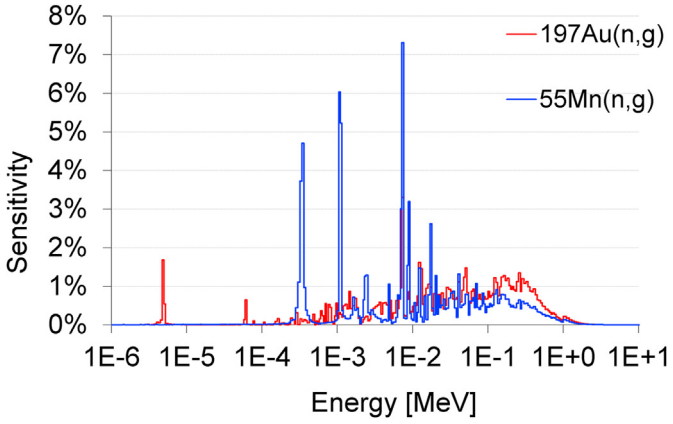

Fig. 10. ^{65}Cu(n,inl) reaction cross section in different libraries.

improvement against ENDF/B-VII.1. Other libraries were not considered there. Furthermore, the neutron spectra were calculated at the place of the copper reflector adjacent to the reactor zone. The place was selected since we expected the most influence of copper there. There are significant differences among criticality predictions in various libraries, namely in the neutron flux in the reflector, as can be seen from Fig. 11.

The higher neutron flux in the reflector the higher is the contribution of the reflector to the total neutron flux in the reactor.

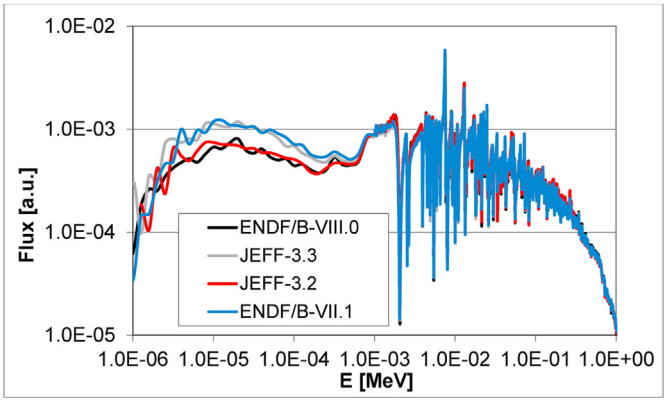

Fig. 11. Comparison of calculated neutron spectra in various libraries. It displays flux normalized to the one fission neutron.

Table 7
Calculation of criticality for various copper cross sections.

	k_{eff}	Uncertainty
ZEUS Case 1	1.00000	0.00240
ENDF/B-VII.1	1.00708	0.00019
ENDF/B-VIII.0	0.99812	0.00019
JEFF-3.3	1.01145	0.00019
JEFF-3.2	1.00681	0.00019

This better slowing down properties seems to manifest itself in higher capture reaction rate in the gold. It is reflected by the fact that ENDF/B-VII.1 library gives higher capture reaction rate and thus higher criticality than ENDF/B-VIII.0 library.

4. Conclusions

The performed experiment reveals necessity of further improvement of copper cross sections. The experiment measured five neutron dosimeter foils ^{58}Ni(n,p)^{58}Co, ^{93}Nb(n,2n)^{92m}Nb, ^{197}Au(n,g)^{198}Au and ^{55}Mn(n,g)^{56}Mn reactions that allow to judge the quality of the evaluated copper transport data. In the resonance and thermal region, the agreement is reasonable for all libraries except CENDL-3.1. In the fast energy region, the differences among libraries are higher and depend on the energy region. The worst agreement is achieved with JEFF-3.3 library. Furthermore, criticality calculations are in the best agreement when using ENDF/B-VIII.0 library against JEFF libraries.

Declaration of competing interest

The authors declare that they have no known competing financial interests or personal relationships that could have appeared to influence the work reported in this paper.

Acknowledgements

The presented work has been realized within Institutional Support by the Ministry of Industry and Trade and with the use of the infrastructure Reactors LVR-15 and LR-0, which is financially supported by the Ministry of Education, Youth and Sports - projectLM2015074, the SANDA project funded under H2020-EURATOM-1.1 contract 847552.

References

[1] S. Singh, M. Kumar, G.P.S. Sodhi, R.K. Buddu, H. Singh, Development of thick copper claddings on SS316L steel for In-vessel components of fusion reactors and copper-cast iron canisters, Fusion Eng. Des. 128 (2018) 126–137.
[2] B. Rosborg, L. Werme, The Swedish nuclear waste program and the long-term corrosion behaviour of copper, J. Nucl. Mater. 379 (Issues 1–3) (2008) 142–153.
[3] M. Zinet, R. Ghazal, H. Issard, O. Bardon, Spent fuel transportation cask under accidental fire conditions: numerical analysis of gas transport phenomena affecting heat transfer in shielding materials, Prog. Nucl. Energy 117 (2019), 103045.
[4] A. Trkov, P.J. Griffin, S.P. Simakov, L.R. Greenwood, K.I. Zolotarev, R. Capote, et al., IRDFF-II: an updated neutron metrology library, Nucl. Data Sheets 163 (2020) 1–108.
[5] W. Mannhart, Status of the Evaluation of the Neutron Spectrum of ^{252}Cf(sf), IAEA Technical Report INDC(NDS)-0540, IAEA, Vienna, 2008. www-nds.iaea.org/standards-cm-oct-2008/6.PDF.
[6] M. Angelone, D. Flammini, S. Loreti, F. Moro, M. Pillon, R. Villari, Copper benchmark experiment at the Frascati Neutron Generator for nuclear data validation, Fusion Eng. Des. Volumes 109–111 (2016) 843–847.
[7] M. Košťál, M. Schulc, et al., Validation of zirconium isotopes (n, g) and (n,2n) cross sections in a comprehensive LR-0 reactor operative parameters set, Appl. Radiat. Isot. 128 (2017) 92–100.
[8] S. Manojlovic, A. Trkov, Nuclear cross section measurement analysis in the californium-252 spectrum with the Monte Carlo method, in: Conf. Nuclear Energy for New Europe, 2011. Ljubljana, Slovenia, contribution 307.

[9] M. Schulc, M. Kostal, R. Capote, et al., Validation of selected (n,2n) dosimetry reactions in IRDFF-1.05 library, Appl. Radiat. Isot. 143 (2019) 132–140.
[10] M. Schulc, M. Kostal, et al., Validation of IRDFF-II library by means of 252Cf spectral averaged cross sections, Appl. Radiat. Isot. 155 (2020), 108937.
[11] M. Schulc, M. kostal, et al., Application of ^{252}Cf neutron source for precise nuclear data experiments, Appl. Radiat. Isot. 151 (2019) 187–195.
[12] T. Goorley, et al., Initial MCNP6 release Overview, Nucl. Tech. 180 (2012) 298–315.
[13] D.A. Brown, M.B. Chadwick, R. Capote, et al., ENDF/B-VIII.0.0: the 8th major release of the nuclear reaction data library with CIELO-project cross sections, new standards and thermal scattering data, Nucl. Data Sheets 148 (2018) 1–142.
[14] M.B. Chadwick, M. Herman, P. Obložinský, et al., ENDF/B-VII.1: nuclear data for science and technology: cross sections, covariances, fission product yields and decay data, Nucl. Data Sheets 112 (2011) 2887–2996.
[15] A.J.M. Plompen, O. Cabellos, C. De Saint Jean, M. Fleming, A. Algora, M. Angelone, et al., The joint evaluated fission and fusion nuclear data library, JEFF-3.3, European Phys. J. A 56 (7) (2020).
[16] A.J. Koning, et al., Status of the JEFF nuclear data library, in: Proceedings of the International Conference on Nuclear Data for Science and Technology, Jeju Island, Korea, 2010, p. 1057.
[17] K. Shibata, O. Iwamoto, T. Nakagawa, N. Iwamoto, A. Ichihara, S. Kunieda, S. Chiba, K. Furutaka, N. Otuka, T. Ohsawa, T. Murata, H. Matsunobu, A. Zukeran, S. Kamada, J. Katakura, JENDL-4.0: a new library for nuclear science and engineering, J. Nucl. Sci. Technol. 48 (2011) 1–30.
[18] Z.G. Ge, Y.X. Zhuang, T.J. Liu, J.S. Zhang, H.C. Wu, Z.X. Zhao, H.H. Xia, The updated version of Chinese evaluated nuclear data library (CENDL-3.1), in: Proc. International Conference on Nuclear Data for Science and Technology, April 2010, pp. 26–30. Jeju Island, Korea.
[19] C. L Dunford, Evaluated nuclear data file, ENDF/B-vi, in: S.M. Qaim (Ed.), Nuclear Data for Science and Technology. Research Reports in Physics, Springer, Berlin, Heidelberg, 1992, https://doi.org/10.1007/978-3-642-58113-7_222.
[20] A. Shaw, F. Rahnema, A. Holcomb, D. Bowen, ENDF/B-VIII.0 CROSS SECTION TESTING FOR COPPER NUCLEAR CRITICALITY SAFETY APPLICATIONS, PHYSOR 2020: Transition to a Scalable Nuclear Future Cambridge, United Kingdom, 2020. March 29th-April 2nd.